Supplementary materials for "FLT1-enriched extracellular vesicles induce a positive feedback loop between nasopharyngeal carcinoma cells and endothelial cells to promote angiogenesis and tumour metastasis"

Supplementary Figures

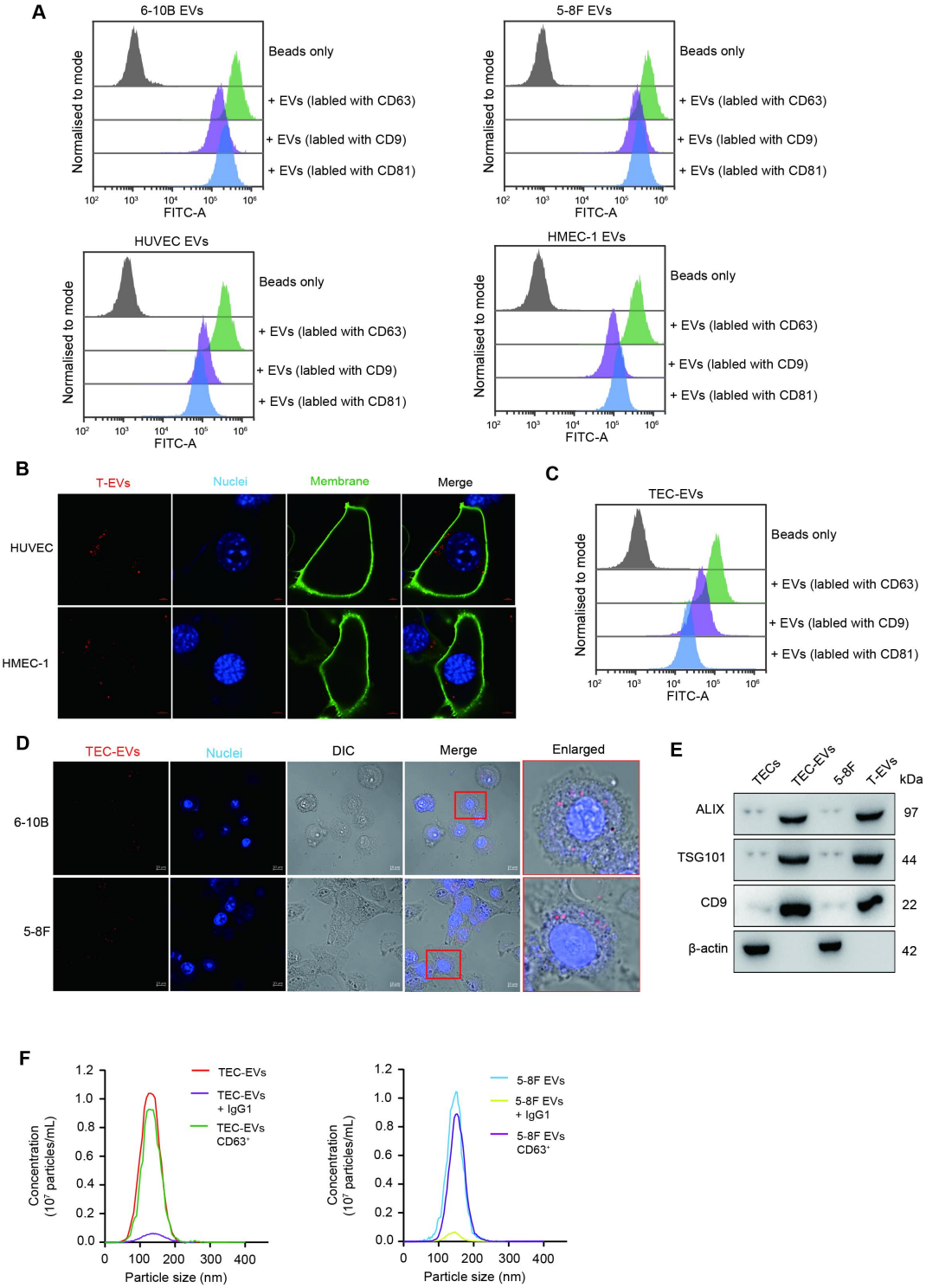

Fig. S1 Characterization of EVs from NPC cells and endothelial cells. A Flow cytometry

analysis of CD63, CD9, and CD81 in purified EVs. **B** Confocal microscopic image showing endothelial cells internalizing DiR-labelled EVs (red) from NPC cells (scale bar, 5 μm). **C** Flow cytometry analysis of CD63, CD9, and CD81 in purified TEC-EVs. **D** Confocal microscopic image showing NPC cells internalizing DiR-labelled EVs (red) from TECs (scale bar, 10 μm). DIC, differential interference contrast. **E** Western blot analysis of CD9, ALIX, and TSG101 in EVs isolated by size-exclusion chromatography. **F** Fluorescence NTA plots illustrating the size distribution and total number of EVs isolated by size-exclusion chromatography with CD63 labeling.

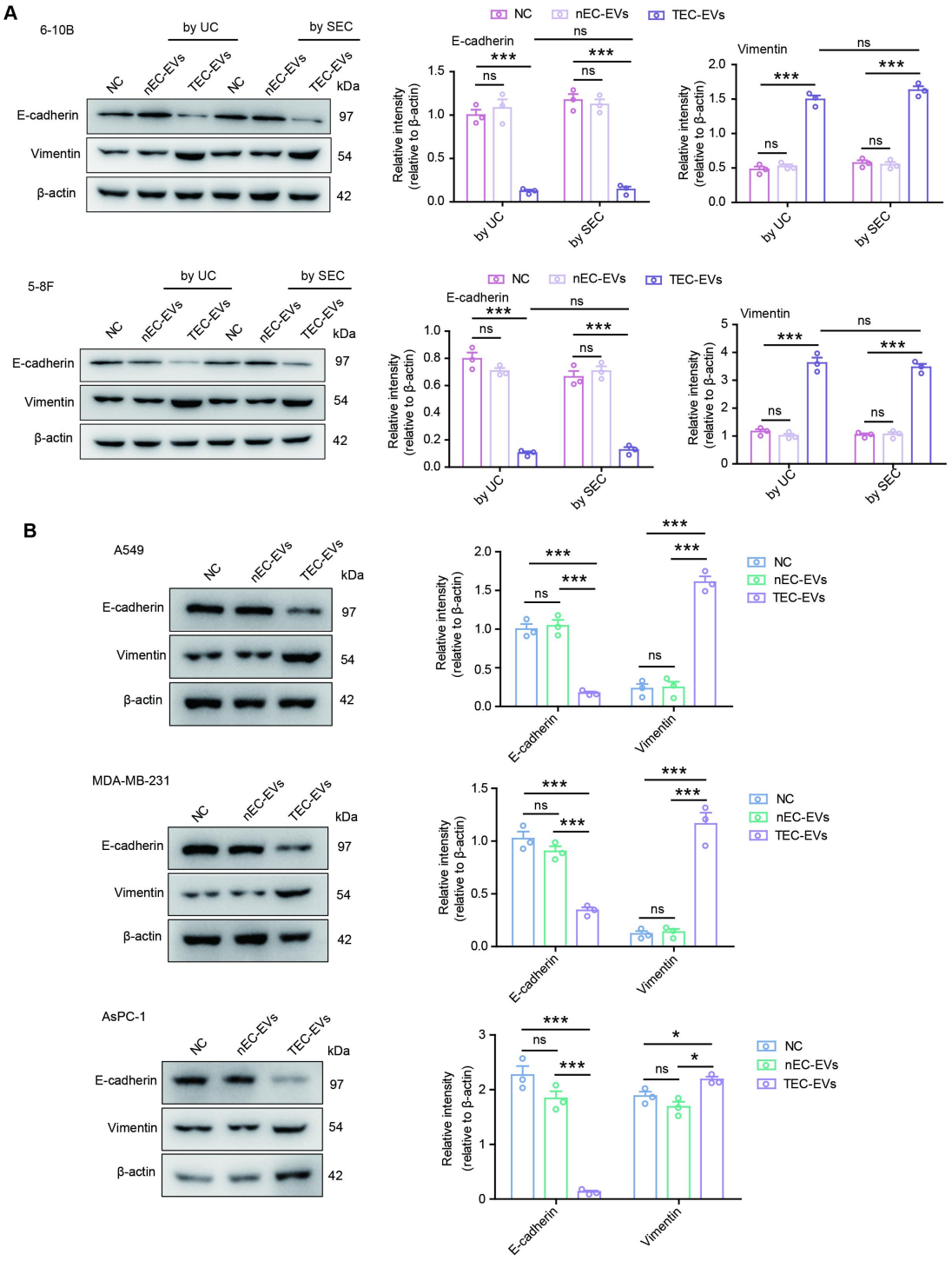

Fig. S2 TEC-derived EVs promote EMT process of tumour cells. A Western blot analysis of E-cadherin and vimentin in NPC cells after treatment with ultracentrifugation (UC) or size-exclusion chromatography (SEC) isolated nEC-EVs (5 μg/ml) or TEC-EVs (5 μg/ml). **B** Western blot analysis of E-cadherin and vimentin in the human lung cancer cell line A549, the

breast cancer cell line MDA-MB-231, and the pancreatic cancer cell line AsPC-1 after treatment with nEC-EVs or TEC-EVs. The E-cadherin/GAPDH and vimentin/GAPDH densitometric ratios were recorded.

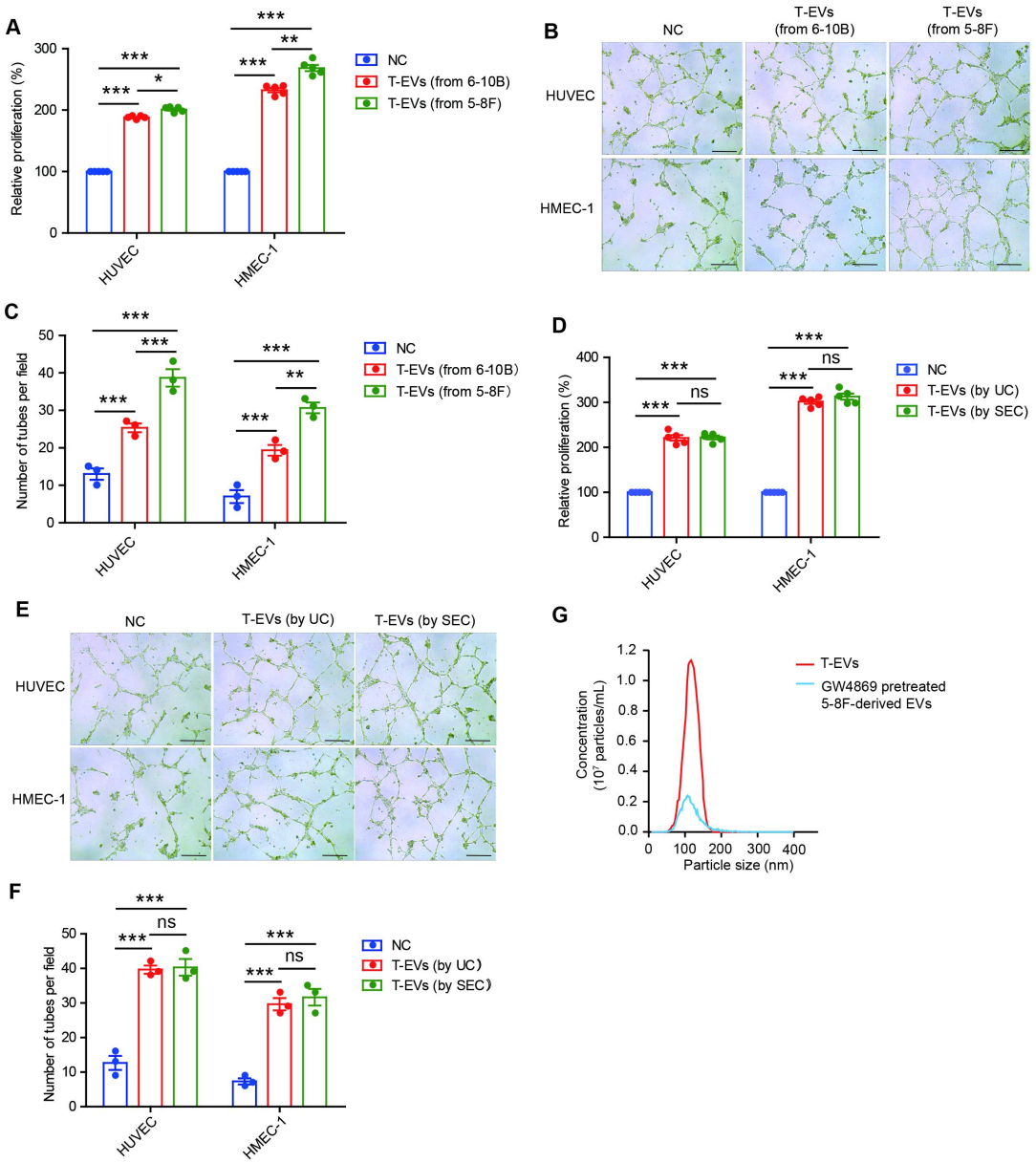

Fig. S3 T-EVs from 6-10B and 5-8F cells promote the proliferation and angiogenesis of endothelial cells. A Cell proliferation of 6-10B- and 5-8F-derived T-EV-treated HUVEC and HMEC-1 cells using CCK-8 assay. **B, C** Tube forming ability of 6-10B- and 5-8F-derived T-EV-treated HUVEC and HMEC-1 cells using tube formation assays (Scale bar, 200 μm). **D** Cell proliferation of HUVEC and HMEC-1 cells treated with T-EVs (5 μg/ml) isolated via UC or SEC was assessed using the CCK-8 assay. **E, F** Tube forming ability of HUVEC and HMEC-1 cells treated with T-EVs (5 μg/ml) isolated via UC or SEC was assessed using tube formation assays

(Scale bar, 200 μm). **G** NTA plots illustrating the size distribution and total number of EVs isolated from GW4869-pretreated 5-8F cells.

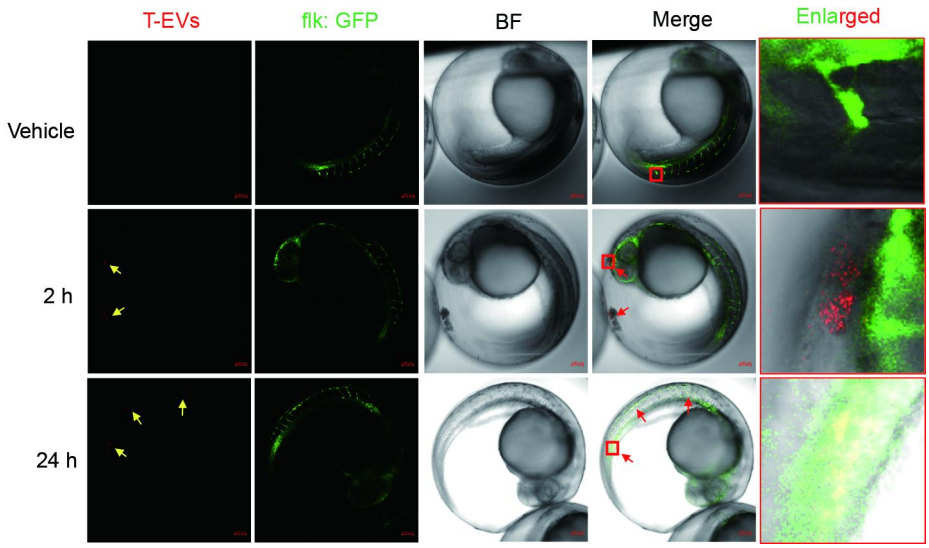

Fig. S4 Confocal microscopy showing zebrafish embryos internalizing PKH26-labelled T-EVs.

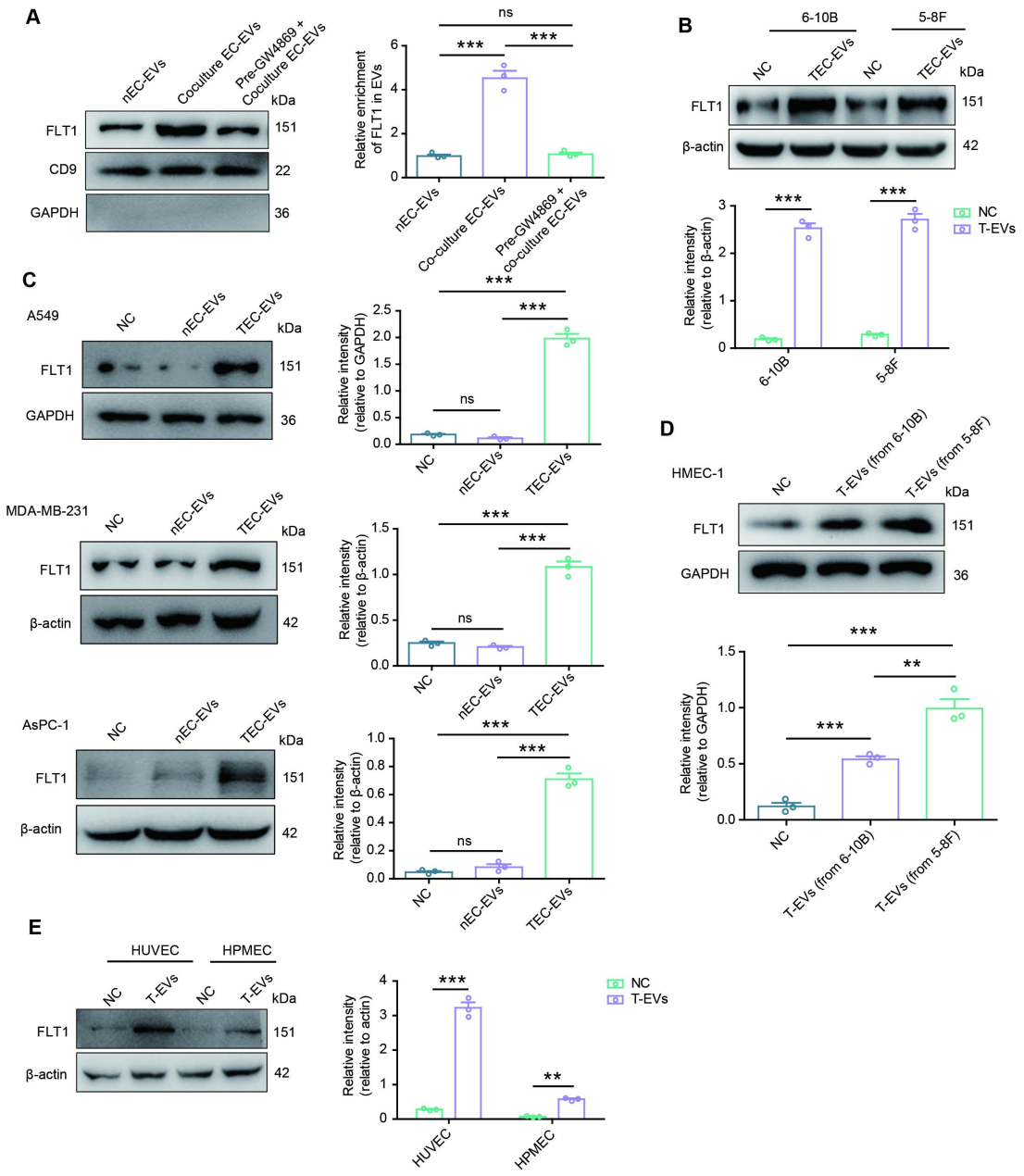

Fig. S5 EV-mediated intercellular communication increases FLT1 in both endothelial cells and NPC cells via transfer of the FLT1 protein. A Western blot for FLT1 enrichment in equal amounts of nEC-EVs, 5-8F cocultured HMEC-1 derived EC-EVs, and GW4869 pretreated 5-8F cocultured HMEC-1 derived EC-EVs. FLT1/CD9 densitometric ratios were recorded. **B** Western blot for FLT1 expression in T-EV-treated NPC. **C** Western blot analysis for FLT1 expression in A549, MDA-MB-231, and AsPC-1 after treatment with nEC-EVs or TEC-EVs. FLT1/GAPDH densitometric ratios were recorded. **D** Western blot analysis for FLT1 expression in HMEC-1 after

treatment with T-EVs derived from 6-10B or 5-8F cells. **E** Western blot analysis for FLT1 expression in HUVEC and human pulmonary microvascular endothelial cells HPMEC after treatment with T-EVs 5-8F cells.

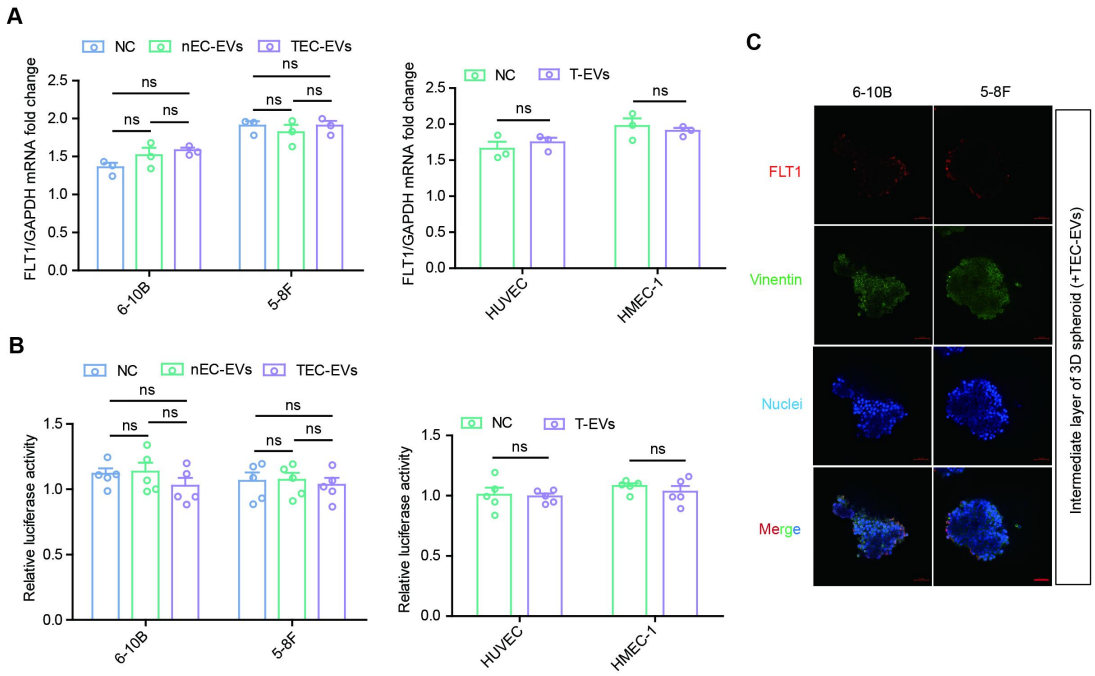

Fig. S6 EV-mediated intercellular communication between endothelial cells and NPC cells has no effect on FLT1 transcription levels. A Relative transcription levels of FLT1 in NPC cells and endothelial cells after treatment with TEC-EVs or T-EVs, respectively, was detected by qRT-PCR. **B** Dual-luciferase assays showing the luciferase activity of NPC cells and endothelial cells transfected with the pmir-GLO-FLT1 promoter and subsequently treated with TEC-EVs or T-EVs. **C** Intermediate layers of 3D spheroids (Scale bar, 50 μm).

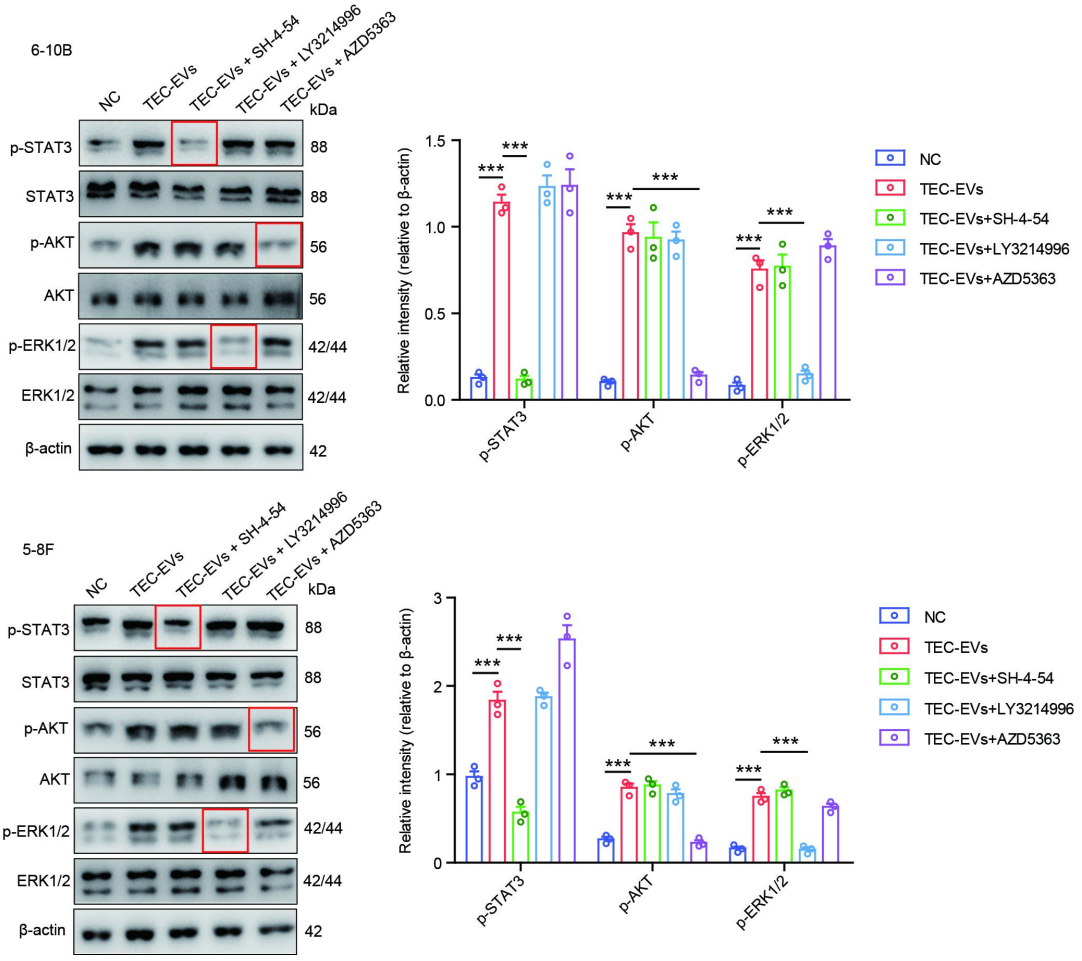

Fig. S7 Western blot analysis of phospho-STAT3, STAT3, phospho-AKT, AKT, phospho-ERK1/2, and ERK1/2 in TEC-EV-treated NPC cells, as well as in NPC cells cotreated with TEC-EVs and SH-4-54, TEC-EVs and LY3214996, and TEC-EVs and AZD5363. The phospho-STAT3/β-actin, phospho-AKT/β-actin, and phospho-ERK1/2/β-actin densitometric ratios were recorded.

Table S1. Information of antibodies used in this study

Antibody	Corporation	Cat.No.	Antibody	Corporation	Cat.No.
anti-E-cadherin	Abcam	ab40772	anti-phospho-ERK1/2	Abcam	ab76299
anti-Vimentin	Abcam	ab20346	anti-ERK1/2	Abcam	ab54230
anti-FLT1	Abcam	Ab32152	anti-phospho-AKT	Abcam	ab8933
anti-FLT1	Abcam	Ab2350	anti-AKT	Abcam	ab179463
anti-CD63	Abcam	ab134045	anti-CD9	Abcam	ab236630
anti-phospho-STAT3	Abcam	ab267373	anti-ALIX	Abcam	ab186728
anti-STAT3	Abcam	ab68153	anti-TSG101	Abcam	ab125011
anti-Ki-67	Abcam	ab92742	anti-VE-Cadherin	Abcam	ab313632
anti-JAM-A	Abcam	ab52647	anti-β-actin	Abcam	ab6276
anti-CD14	Abcam	ab314062	anti-CD105	Abcam	ab2529
anti-CD34	Abcam	ab81289	anti-CD45	Abcam	ab40763
anti-CD31	Abcam	ab9498	anti-GAPDH	Abcam	ab8245
anti-CD64	Abcam	ab288731	anti-CD63	Abcam	ab18235
anti-CD9	Abcam	ab18241	anti-CD81	Abcam	ab239256
anti-CD63	Abcam	ab315108			